

A Mitigation Technique for Inrush Currents in Load Transformers for the Series Voltage Sag Compensator

B.Hari Prasad ¹, P.Harsha Vardhan Reddy ¹, Dr.M.Padma Lalitha ^{*1}

Received 24th July 2013, Accepted 17th November 2013

Abstract: In many countries, high-tech manufacturers concentrate in industry parks. Survey results suggest that 92% of interruption at industrial facilities is voltage sag related. An inrush mitigation technique is proposed and implemented in a synchronous reference frame sag compensator controller. The voltage sag compensator consists of a three phase voltage source inverter and a coupling transformer for serial connection. It is the most cost effective solution against voltage sags. When voltage sag happen, the transformers, which are often installed in front of critical loads for electrical isolation, are exposed to the disfigured voltages and a DC offset will occur in its flux linkage. When the compensator restores the load voltage, the flux linkage will be driven to the level of magnetic saturation and severe inrush current occurs. The compensator is likely to be interrupted because of its own over current protection. This paper proposes an inrush current mitigation technique together with a state-feedback controller for the Voltage sag compensator.

Keywords: Voltage sag, flux linkage, inrush current, transformer, power quality, voltage sag compensator.

1. Introduction

Power quality issues have received much attention in recent years. Therefore, any power quality events in the utility grid can affect a large number of manufactures. Records show that voltage sag, transients, and momentary interruption constitute 92% of the power quality problems [1]. Voltage sags often interrupt critical loads and results in substantial productivity losses. Industries have adopted the voltage sag compensators as one of the most cost-effective ride-through solutions [2]–[7], and most compensators can accomplish voltage restoration within a quarter cycles. However, the load transformer is exposed under the deformed voltages before the restoration, and magnetic flux deviation may be developed within the load transformers. Once the load voltage is restored, the magnetic flux may further drift beyond the saturation knee of the core and lead to significant inrush current. The over current protection of the compensator could be easily triggered and lead to compensation failure. Various transformer inrush reduction techniques have been presented, like controlling power-on angle and the voltage magnitude [8], or actively controlling the transformer current [9]. These methods could easily alter the output voltage waveforms of the converter, and thus, is not suitable for voltage sag compensators, which demand precise point-on wave restoration of the load voltages.

2. Compensator Configuration.

The voltage sag compensator consists of a three-phase voltage-source inverter (VSI) and a coupling transformer for serial connection as shown in Fig.1.

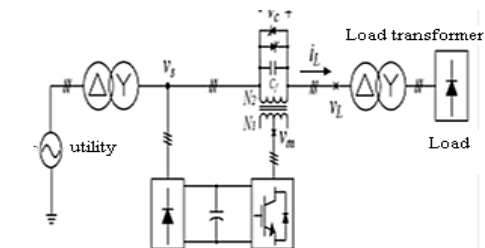


Figure 1. Simplified one Line diagram of the off line series voltage sag compensator

When the grid is normal, the compensator is bypassed by the thyristors for high operating efficiency. When voltage sags occur, the voltage sag compensator injects the required compensation voltage through the coupling transformer to protect critical loads from being interrupted. However, certain detection time (typically within 4.0 ms) is required by the sag compensator controller to identify the sag event [10]. And the load transformer is exposed to the deformed voltage from the sag occurrence to the moment when the compensator restores the load voltage. Albeit its short duration, the deformed voltage causes magnetic flux deviation inside the load transformer, and the magnetic saturation may easily occur when the compensator restores the load voltage, and thus, results in the inrush current. The inrush current could trigger the over current protection of the compensator and lead to compensation failure. Thus, this paper proposes an inrush mitigation technique by correcting the flux linkage offsets of the load transformer, and this technique can be seamlessly integrated with the state-feedback controller of the compensator.

2.1. Dynamics of the Sag Compensator.

The dynamics of the sag compensator can be represented by an equivalent circuit in Fig.2. Generally, the sag compensator is rated for

¹ Department of Electrical & Electronics Engineering, Annamacharya Institute of Technology & science, India

* Corresponding Author: Email: poredyharshavardhan@gmail.com

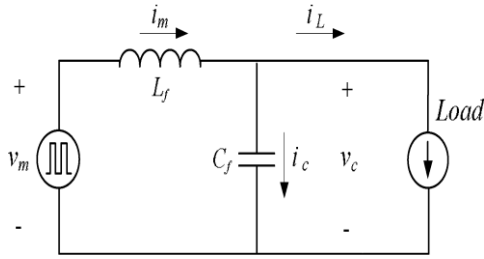


Figure 2. Per-phase equivalent circuit of the series voltage sag compensator

Compensating all three phase voltages down to 50% of nominal grid voltage. The coupling transformer is capable of electrical isolation or boosting the compensation voltage. Moreover, the leakage inductor of the coupling transformer is used as the filter inductor L_f and is combined with the filter capacitor C_f installed in the secondary winding of the coupling transformer to suppress pulse width modulated (PWM) ripples of the inverter output voltage v_m . The dynamics equations are expressed as follows

$$L_f \frac{d}{dt} \begin{bmatrix} i_{ma} \\ i_{mb} \\ i_{mc} \end{bmatrix} = \begin{bmatrix} v_{ma} \\ v_{mb} \\ v_{mc} \end{bmatrix} - \begin{bmatrix} v_{ca} \\ v_{cb} \\ v_{cc} \end{bmatrix} \quad (1)$$

$$C_f \frac{d}{dt} \begin{bmatrix} v_{ca} \\ v_{cb} \\ v_{cc} \end{bmatrix} = \begin{bmatrix} i_{ma} \\ i_{mb} \\ i_{mc} \end{bmatrix} - \begin{bmatrix} i_{La} \\ i_{Lb} \\ i_{Lc} \end{bmatrix} \quad (2)$$

Where $[v_{ma} v_{mb} v_{mc}]^T$ is the inverter output voltage, $[i_{ma} i_{mb} i_{mc}]^T$ is the filter inductor current, $[v_{ca} v_{cb} v_{cc}]^T$ is the compensation voltage, and $[i_{La} i_{Lb} i_{Lc}]^T$ is the load current. Equations (1) and (2) are transformed into the synchronous reference frame as the following:

$$\frac{d}{dt} \begin{bmatrix} i_{mq}^e \\ i_{md}^e \end{bmatrix} = \begin{bmatrix} 0 & -\omega \\ \omega & 0 \end{bmatrix} \begin{bmatrix} i_{mq}^e \\ i_{md}^e \end{bmatrix} + \frac{1}{L_f} \begin{bmatrix} v_{mq}^e \\ v_{md}^e \end{bmatrix} - \frac{1}{L_f} \begin{bmatrix} v_{cq}^e \\ v_{cd}^e \end{bmatrix} \quad (3)$$

$$\frac{d}{dt} \begin{bmatrix} v_{cq}^e \\ v_{cd}^e \end{bmatrix} = \begin{bmatrix} 0 & -\omega \\ \omega & 0 \end{bmatrix} \begin{bmatrix} v_{cq}^e \\ v_{cd}^e \end{bmatrix} + \frac{1}{C_f} \begin{bmatrix} i_{mq}^e \\ i_{md}^e \end{bmatrix} - \frac{1}{C_f} \begin{bmatrix} i_{Lq}^e \\ i_{Ld}^e \end{bmatrix} \quad (4)$$

where superscript “e” indicates the synchronous reference frame representation of this variable and ω is the angular frequency of the utility grid. Equations (3) and (4) show the cross-coupling terms between the compensation voltage and the filter inductor current. The block diagram of the physical circuit dynamics are illustrated in the right-hand side of Fig.3.

2.2. Voltage and Current Closed-Loop Controls

Fig.3 shows the block diagram of the proposed control method. Note that the d-axis controller is not shown for simplicity. The block diagram consists of the full state-feedback controller [12] and the proposed inrush current mitigation technique. The feedback control, feed forward control, and decoupling control are explained as follows.

1) Feedback Control: The feedback control is to improve the precision of the compensation voltage, the disturbance rejection capability, and the robustness against parameter variations. As shown in Fig.3, the capacitor voltage v_{cq}^e and the inductor current i_{mq}^e are handled by the outer-loop voltage control and the inner-loop current control, respectively. The voltage control is implemented by a proportional gain K_{pv} with a voltage command v_{cq}^{*e} produced by the voltage sag compensation scheme. The current control also consists of a proportional control gain K_{pi} to accomplish fast current tracking.

2) Feed forward Control: To improve the dynamic response of the

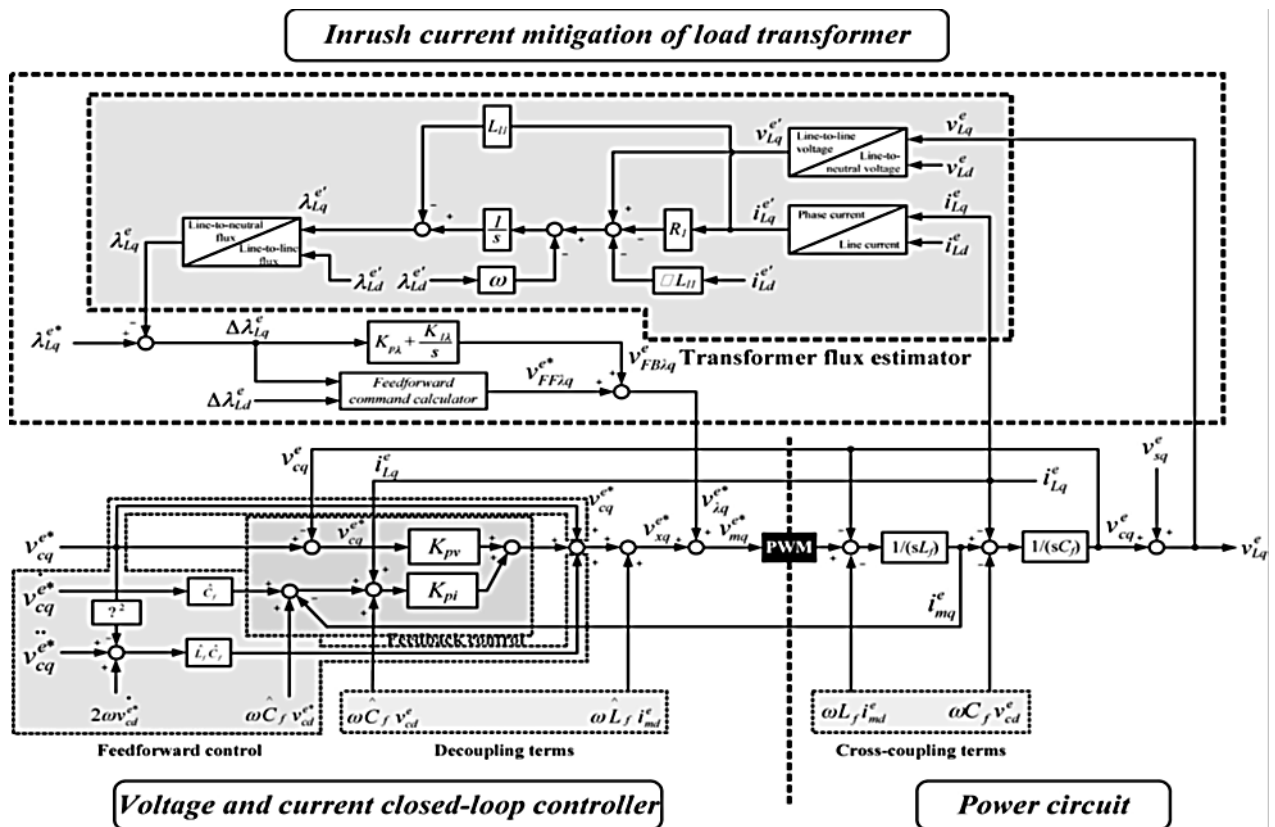


Figure 3. Block diagram of the proposed inrush current mitigation technique with the state-feedback control

voltage sag compensator, the feed forward control is added to the voltage controller to compensate the load voltage immediately when voltage sag occurs. The feed forward voltage command can be calculated by combining the compensation voltage and the voltage drop across the filter inductor L_f .

3) Decoupling Control: The cross-coupling terms are the result of the synchronous reference frame transformation, as in (3) and (4). The controller utilizes the decoupling terms to negate the cross coupling and reduce the interferences between the d-q axes. Fig. 3 shows that the decoupling terms can be accomplished by the filter capacitor voltage v_{cd} , the filter inductor current i_{md} and the estimated values of the filter capacitor and the filter inductor.

2.3. Inrush Current Mitigation Technique

1) Flux Linkage Deviation due to Sags: The flux linkage of the phase a and b winding is expressed as follows:

$$\lambda_{Lab}(t) = \int v_{Lab}(\tau) d\tau \quad (5)$$

Fig.5. illustrates the line-to-line voltage across the transformer winding and the resulting flux linkage from the sag occurrence to completion of the voltage compensation. When voltage sag occurs ($t=t_{sag}$), The controller detects the sagged voltage and injects the required compensation voltage at $t = t_{action}$. The flux linkage of the transformer winding a and b during the voltage compensation process can be expressed as following:

where v_{Lab}^* is the normal load voltage defined as follows

$$\lambda_{Lab}(t) = \lambda_{Lab}(t)_{t=t_{sag}} + \int_{t_{sag}}^{t_{action}} v_{Lab}(\tau) d\tau + \int_{t_{action}}^t v_{Lab}^*(\tau) d\tau \quad (6)$$

$$v_{Lab}^*(t) = v_{Lab}^* \sin(\omega t + \phi_{Lab}^*)$$

Equation (6) can be rewritten as follows:

$$\lambda_{Lab}(t) = \lambda_{Lab}(t)_{t=t_{sag}} - \int_0^{t_{sag}} v_{Lab}(\tau) d\tau + \int_{t_{sag}}^{t_{action}} (v_{Lab}(\tau) - v_{Lab}^*(\tau)) d\tau + \int_0^t v_{Lab}^*(\tau) d\tau \quad (7)$$

where v_{Lab}^* is the magnitude of load voltage, ω is the grid frequency, and ϕ_{Lab}^* is the phase angle. Thus, after the voltage compensation is completed, the flux linkage can be expressed as follows:

$$\lambda_{Lab}(t) = \Delta\lambda_{Lab}(t)_{t=t_{action}} + \frac{v_{Lab}^*}{\omega} \sin\left(\omega t + \phi_{Lab}^* - \frac{\pi}{2}\right) \quad (8)$$

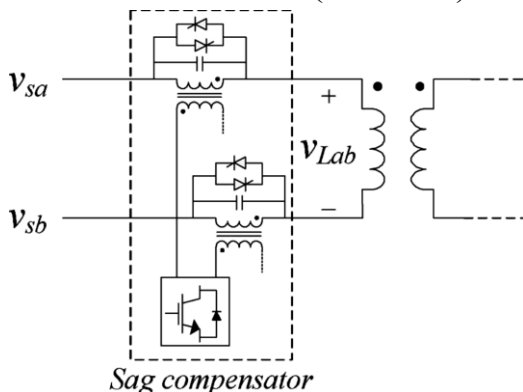


Figure 4. Connection diagram of the proposed system and the delta/wye load transformer

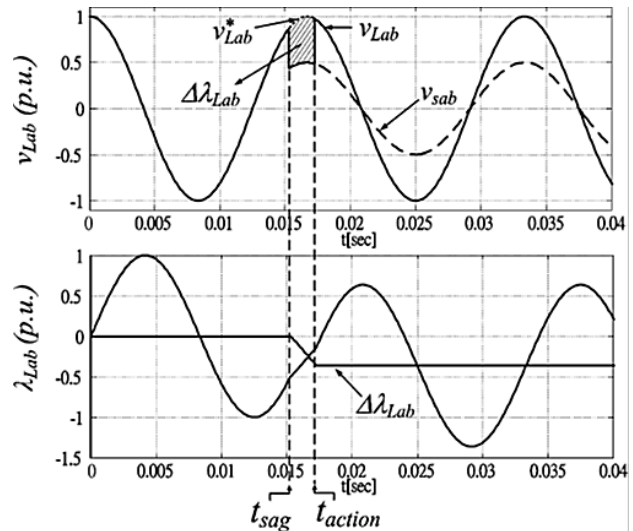


Figure 5. Transformer voltage and corresponding transient flux linkage

2) Design of the Flux Linkage Estimator: Fig.6 is a per phase model of a three-phase transformer under load, where R_1 and R_2 represent the copper losses, L_{11} and L_{12} are the equivalent leakage inductances, R_c represents the core losses, and L_m is the magnetizing inductance.

The dynamics equation of the load transformer can be represented in the synchronous reference frame as follows:

$$s \begin{bmatrix} \lambda_{mq}^e \\ \lambda_{md}^e \end{bmatrix} = \begin{bmatrix} v_{Lq}^e \\ v_{Ld}^e \end{bmatrix} - (R_1 + L_{11})s \begin{bmatrix} i_{Lq}^e \\ i_{Ld}^e \end{bmatrix} - L_{11} \begin{bmatrix} 0 & \omega \\ -\omega & 0 \end{bmatrix} \begin{bmatrix} i_{Lq}^e \\ i_{Ld}^e \end{bmatrix} - \begin{bmatrix} 0 & \omega \\ -\omega & 0 \end{bmatrix} \begin{bmatrix} \lambda_{Lq}^e \\ \lambda_{Ld}^e \end{bmatrix} \quad (9)$$

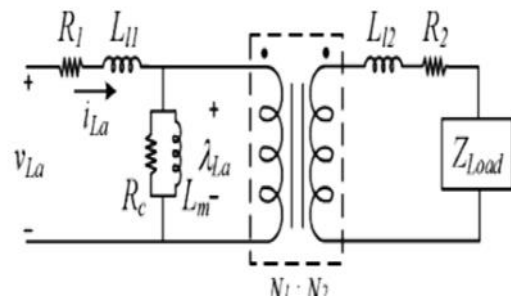


Figure 6. Equivalent per-phase circuit model of the load transformer

where the frequency ω (≈ 377 rad/s) is the angular frequency of the utility grid. A flux linkage estimator based on (9) can be implemented, as shown in Fig. 7. This transformer flux estimation scheme is applied to the proposed inrush mitigation technique, which includes the feedback and feed forward control of the flux linkage. The integration of voltage and current closed-loop controllers and the transformer flux estimator are shown in Fig.3. In the control block diagram, the flux estimator is used for the load transformer with delta-wye connection. Thus, a transformation from the line-to-neutral voltage to the line-to-line voltage is applied to obtain the voltages across the transformer windings. In practical applications, moreover, the integrator in the proposed flux estimator is usually implemented as the low-pass filter with an extremely low cutoff frequency ($1/(s + \omega_c)$) to provide stability and avoid any accumulative errors caused by the signal offset from the transducers and the analog/digital converters. In the feedback control loop, the flux linkage command λ_{Lq}^* is calculated based

on pre fault load voltage v_{Lq}^e , and the estimated flux linkage λ_{Lq}^e is generated by the flux linkage estimator in Fig.7. The error between λ_{Lq}^{e*} and λ_{Lq}^e is regulated by a PI regulator. To speed up the dynamics response of the inrush current mitigation, the estimated flux linkage deviation $\Delta\lambda_{Lq}^e (= \lambda_{Lq}^{e*} - \lambda_{Lq}^e)$ is also utilized as a feed forward control term. The feed forward command calculator can generate a suitable feed forward flux command according to the estimated flux linkage deviation $\Delta\lambda_{Lq}^e$ and $\Delta\lambda_{Ld}^e$ to accelerate the correction of flux linkage during the compensator starting transient. Details of the feed forward command calculator and the design process are given in [11].

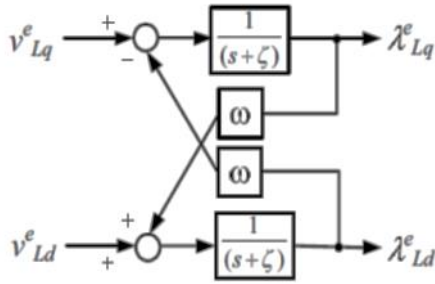


Figure 7. Proposed flux linkage estimator under the synchronous reference frame.

The flux linkage controller eventually produce the voltage command $V_{e\lambda q}$, as shown in Fig.3. The complete command voltages of the sag compensator is established by the summation of $V_{e\lambda q}$ and $V_{e\lambda q}^*$ (from the voltage and current closed-loop control

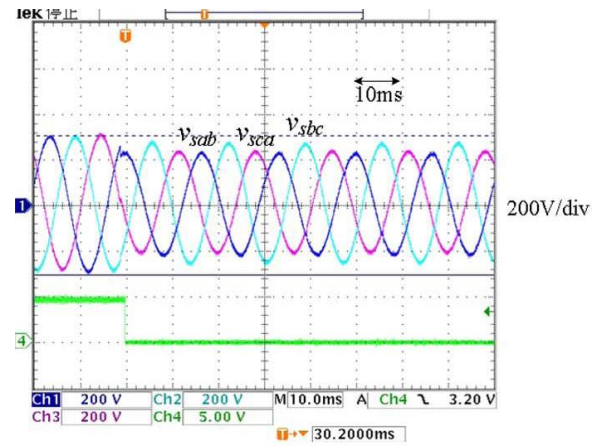
3. Simulation Results

A prototype voltage sag compensator with inrush current mitigation technique is implemented in MATLAB. The one-line diagram is as given in Fig.1.

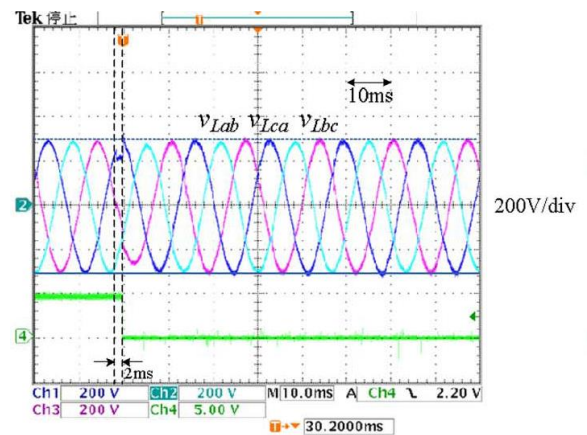
Fig. 8. shows that asymmetrical fault is introduced in utility line, and the simulation results of voltage sag compensator without the inrush current mitigation technique. The controller detects the voltage sag in 4.0ms after the fault occurs, and injects the required compensation voltage immediately to maintain load voltage in normal value as shown in Fig. 8(b). The transformer flux linkage DC offsets caused by the voltage sag can be clearly observed in Fig. 8(c), which results in a significant inrush current of peak value 14A as shown in Fig. 8(d). Fig. 8(e) shows the transformer flux linkage under the synchronous reference frame (λ_{eLd}). The voltage compensation process causes the flux linkage λ_{eLd} oscillate and naturally decays to the normal state by core losses of the transformer and the power consumption of the load.

Under the same asymmetrical fault, Fig. 9 shows the simulation waveforms when the inrush current mitigation technique is utilized in compensation process. Fig. 9(a) and (b) illustrate proposed inrush current mitigation technique can achieve fast voltage compensation and without any flux linkage DC offset during the transient compared with Fig. 8(b) and (c). Therefore, the inrush current caused by the voltage sag can be avoided completely compared to Fig. 8(d). Furthermore, Fig. 9(a) also shows that the inrush current mitigation technique generates an extra voltage to correct the trace of transient flux linkage when the compensation is initiated compared to Fig. 8(c). The magnitude of the extra voltage is usually dependent on proportion gain $KP\lambda$. Fig.9(d) shows the tracking performance of proposed inrush current mitigation technique. The P-I regulator proposed method can be recognized as a virtual damper. A large number of KP can

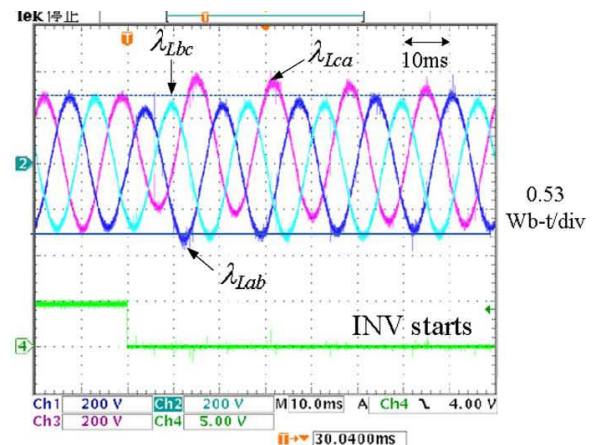
accelerate the flux linkage λ_{Ld} to track the flux linkage command λ_{Ld}^{e*} . However, it may cause a high current in the start transient.



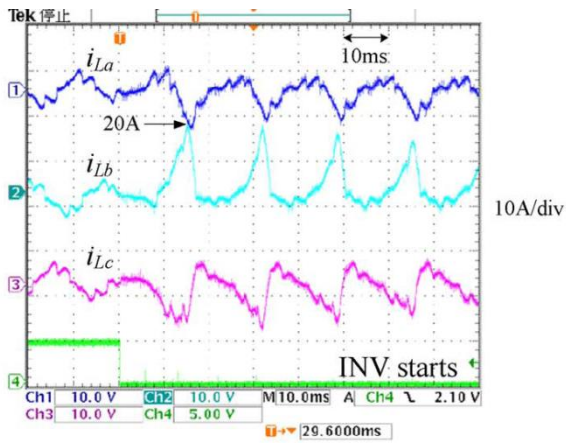
(a)



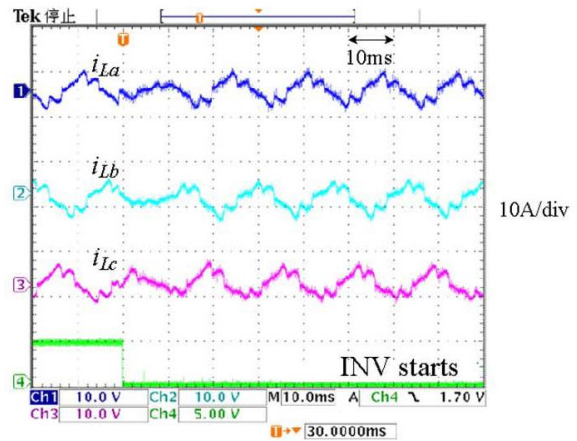
(b)



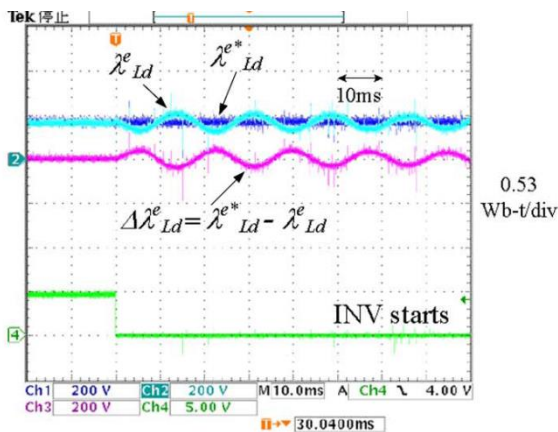
(c)



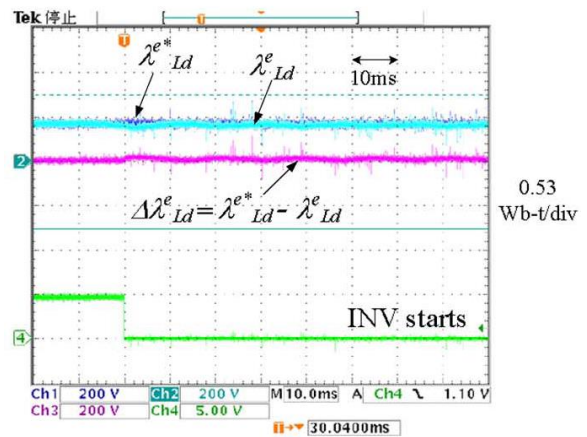
(d)



(c)



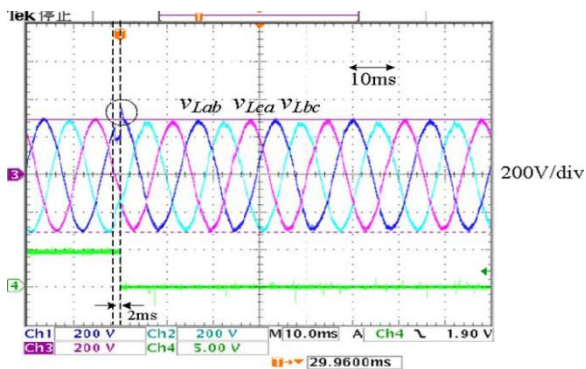
(e)



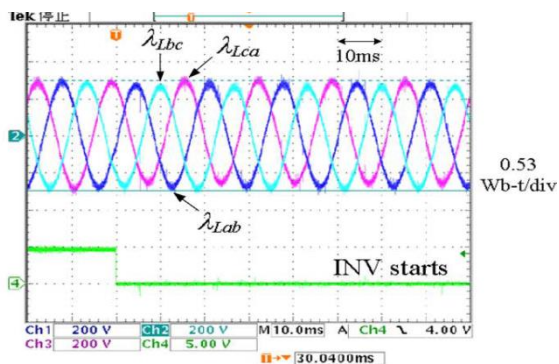
(d)

Figure 8. Test results under phase to phase voltage sag without the proposed inrush current mitigation technique. (a) Source voltage V_s . (b) Load voltage V_{L-L} . (c) Flux linkage of the load transformer λ_{L-L} . (d) Load current I_L . (e) Flux linkage of d-axis λ^e_{Ld} .

Figure 9. Test results under a phase to phase voltage sag with the inrush current mitigation technique. (a) Load voltage V_{L-L} . (b) Flux linkage of the load transformer λ_{L-L} . (c) Load current I_L . (d) Flux linkage of d-axis λ^e_{Ld} .



(a)



(b)

4. Conclusion

This paper proposes an inrush current mitigation technique incorporating with the full state feedback controller to prevent the inrush current during the voltage compensation process. The controller includes a voltage control, a current control and a flux linkage control. The proposed control method is based on the synchronous reference frame which enables voltage sag compensator to achieve fast voltage injection and prevent the inrush current. When voltage sag occurs, the controller can track the transient flux linkage and calculate a required compensation voltage in real-time for fast compensation and elimination of flux linkage DC offset caused by voltage sags. It shows that the proposed control method provides a high disturbance rejection capability for voltage sag compensator compared with conventional voltage-current state feedback control method. The proposed method can be easily integrated with the existing voltage sag compensation control system without using any extra sensors.

References

- [1] D. L. Brooks and D. D. Sabin, "An assessment of distribution system power quality," Elect. Power Res. Inst., Palo Alto, CA, EPRI Final Rep. TR-106249-V2, May 1996, vol. 2.
- [2] W. E. Brumsickle, R. S. Schneider, G. A. Luckjiff, D. M. Divan, and M. F. McGranaghan, "Dynamic sag correctors: Cost-effective industrial power line conditioning," IEEE

- Trans. Ind. Appl., vol. 37, no. 1, pp. 212–217, Jan./Feb. 2001.
- [3] N. H. Woodley, “Field experience with dynamic voltage restorer (DVRTMMV) systems,” in Proc. IEEE Power Eng. Soc. Winter Meeting, Jan. 23–27, 2000, vol. 4, pp. 2864–2871.
- [4] R. Affolter and B. Connell, “Experience with a dynamic voltage restorer for a critical manufacturing facility,” in Proc. IEEE Transmiss. Distrib. Conf. Expo., 2003, vol. 3, pp. 937–939.
- [5] C. N.-M. Ho, H. S. H. Chung, and K. T. K. Au, “Design and implementation of a fast dynamic control scheme for capacitor-supported dynamic voltage restorers,” IEEE Trans. Power Electron., vol. 23, no. 1, pp. 237–251, Jan. 2008.
- [6] C. Meyer, R. W. De Doncker, Y. W. Li, and F. Blaabjerg, “Optimized control strategy for a medium voltage DVR—Theoretical investigations and experimental results,” IEEE Trans. Power Electron., vol. 23, no. 6, pp. 2746–2754, Nov. 2008.
- [7] J. G. Nielsen and F. Blaabjerg, “A detailed comparison of system topologies for dynamic voltage restorers,” IEEE Trans. Ind. Appl., vol. 41, no. 5, pp. 1272–1280, Sep./Oct. 2005.
- [8] M. S. J. Asghar, “Elimination of inrush current of transformers and distribution lines,” in Proc. IEEE Power Electron., Drives Energy Syst. Ind. Growth, 1996, vol. 2, pp. 976–980.
- [9] Y. Cui, S. G. Abdulsalam, S. Chen, and W. Xu, “A sequential phase energization technique for transformer inrush current reduction—Part I: Simulation and experimental results,” IEEE Trans. Power Del., vol. 20, no. 2, pp. 943–949, Apr. 2005.
- [10] W. Xu, S. G. Abdulsalam, Y. Cui, and X. Liu, “A sequential phase energization technique for transformer inrush current reduction—Part II: Theoretical analysis and design guide,” IEEE Trans. Power Del., vol. 20, no. 2, pp. 950–957, Apr. 2005.
- [11] P. C. Y. Ling and A. Basak, “Investigation of magnetizing inrush current in a single-phase transformer,” IEEE Trans. Magn., vol. 24, no. 6, pp. 3217–3222, Nov. 1988.
- [12] C. Fitzer, A. Arulampalam, M. Barnes, and R. Zurowski, “Mitigation of saturation in dynamic voltage restorer connection transformers,” IEEE Trans. Power Electron., vol. 17, no. 6, pp. 1058–1066, Nov. 2002.